Novel Architecture and MMICs for an Integrated Front End of a Spectrum Analyzer

Tsutomu Takenaka, Atsushi Miyazaki and Hiroyuki Matsuura

TERATEC Corporation

Musashinoshi, Tokyo, Japan

Abstract– This paper proposes a novel architecture and MMICs for an integrated front end of a 2-32 GHz spectrum analyzer. The architecture achieves miniaturization by eliminating the YIG tracking filter. The MMICs achieve ultra-wideband performances as well as chip-size reduction by utilizing novel FET cells for the basic circuit functions.

INTRODUCTION

RF front ends of conventional microwave and millimeter-wave instruments are assembled in main-frames, so access to a device-under-test (DUT) requires interconnections such as co-axial cables, connectors or wave-guides. These interconnections decrease dynamic range and reliabilty of measurement and flexibility in handling; moreover, they sometimes limit the frequency range by imposing a cut-off-frequency. To overcome these problems, active electronic wafer-probes with mounted ICs have been proposed in millimeter-wave sampling applications [1], [2].

This paper proposes a novel architecture and MMICs for integrating a front end of an RF spectrum analyzer in the probe configuration. This architecture eliminates the YIG tracking filter, because its size and weight are not suitable for integration. Multi-octave measurement is also achieved with less than one octave sweep of the first local oscillator (1st LO) frequency by adapting a fundamental and harmonic frequency conversion.

The developed MMICs are a fundamental/harmonic frequency converter, a variable attenuator, a single-pole triple-throw switch, a single-pole double-throw switch, a distributed pre-amplifier and an active LC filter, which are all of the active circuits of the proposed architecture. All the MMICs achieve ultra-wideband performance of 2-32 GHz in a chip size of less than 1 mm^2, except the active LC filter, since they reduce the conventional quarter-wavelength line circuits and stub lines as much as possible by utilizing novel FET cells for basic circuit functions such as power combination, multi-order frequency conversion, low leakage variable resistor,. and active impedance translation. Another feature of the MMICs is a thin film micro-strip line that effectively achieves a highly isolated line-cross-over and flexible allocation of bias distributions on the co-planar wave-guide MMICs.
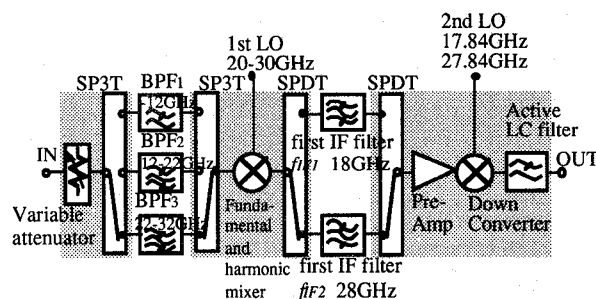

Fig. 1 Novel architecture for the integrated front end of the 2-32GHz spectrum analyzer. MMICs realize the hatched area.

NOVEL ARCHITECTURE OF SPECTRUM ANALYZER

Figure 1 shows a block diagram of the proposed spectrum analyzer architecture. The measurement frequency range is set to 2-32GHz. The block diagram discriminates the frequency spectrum of the input signal by sweeping the 1st LO frequency (f_{LO}) and synchronizing the converted signal of the frequency converter with the pass-frequency of the first IF filter (f_{IF1} and f_{IF2}), and eliminates image responses and IF feedthrough by using a set of bandpass-filters BPF_m optimized by the following procedure:

1. The measurement frequency f_S is given by Eq. (1) when n-th order harmonic conversion is selected,

$$f_s = |nf_{LO} - f_{IFx}| \qquad n = 1,2,3,\cdots,\infty, \quad x=1,2 \qquad (1)$$

2. In condition 1, the range of f_{LO} is

$$f_{LO1} \leq f_{LO} \leq \frac{f_{LO2} - f_{LO1}}{n} + f_{LO1} \qquad (2)$$

where f_{LO1} and f_{LO2} are minimum and maximum frequencies of the 1st LO, respectively.

3. If f_{IFx} is selected for the first IF, an input frequency f_{IFx} should be rejected at the bandpass filter BPF_m ($m=1$ at $n=1$ and $x=1$, $m=2$ at $n=2$ and $x=1$, $m=3$ at $n=2$ and $x=2$,...).

From these conditions, actual frequency conversion formulae and sweep ranges of f_{LO} are represented by:

for BPF_1 $\quad f_s = f_{LO} - f_{IF1}$ with $f_{LO1} \leq f_{LO} \leq f_{LO2}$ (3)

for BPF_2 $\quad f_s = 2f_{LO} - f_{IF2}$

$$\text{with } f_{LO1} \leq f_{LO} \leq \frac{f_{LO2} - f_{LO1}}{2} + f_{LO1} \qquad (4)$$

for BPF_3 $\qquad f_s = 2f_{LO} - f_{IF1}$

$$\text{with } f_{LO1} \leq f_{LO} \leq \frac{f_{LO2} - f_{LO1}}{2} + f_{LO1} \qquad (5)$$

for BPF_4 $\qquad f_s = 3f_{LO} - f_{IF2}$

$$\text{with } f_{LO1} \leq f_{LO} \leq \frac{f_{LO2} - f_{LO1}}{3} + f_{LO1} \qquad (6)$$

$$\vdots \qquad \vdots \qquad \vdots$$

for BPF_m $\qquad f_s = nf_{LO} - f_{IF2}$

$$\text{with } f_{LO1} \leq f_{LO} \leq \frac{f_{LO2} - f_{LO1}}{n} + f_{LO1} \qquad (7)$$

for BPF_{m+1} $\qquad f_s = nf_{LO} - f_{IF1}$

$$\text{with } f_{LO1} \leq f_{LO} \leq \frac{f_{LO2} - f_{LO1}}{n} + f_{LO1} \qquad (8)$$

where $f_{LO1} - f_{IF1} > 0$ and $2f_{LO1} - f_{IF2} > 0$.
The f_s must be continual through Eq. (3)-(8), so we get

$$\frac{f_{LO2}}{f_{LO1}} = 1.5 \qquad (9)$$

From condition 3, f_{IF1} and f_{IF2} must be in the bandwidths of BPF_2 and BPF_3, respectively. When f_{IF1} and f_{IF2} are placed at the centers of those bandwidths, Eqs. (10) and (11) are extracted from Eqs. (3), (5) and Eqs. (4), (6), respectively.

$$f_{IF1} = \frac{f_{LO2}}{4} + \frac{f_{LO1}}{2} \qquad (10)$$

$$f_{IF2} = \frac{f_{LO2}}{4} + f_{LO1} \qquad (11)$$

When the measurement range of 2-32 GHz is applied to Eqs. (3)-(5) and (9)-(11), we can determine all parameters shown as Eq. (12).

$$
\begin{aligned}
f_{LO1} &= 20GHz \\
f_{LO2} &= 30GHz \\
f_{IF1} &= 18GHz \\
f_{IF2} &= 28GHz
\end{aligned}
\qquad
\begin{aligned}
BW_{BPF1} &= 2 \rightarrow 12GHz \\
BW_{BPF2} &= 12 \rightarrow 22GHz \\
BW_{BPF3} &= 22 \rightarrow 32GHz
\end{aligned}
\qquad (12)
$$

In Fig. 1, the lowest bandpass filter BPF_1 is replaced with a low-pass filter. The relationship of f_{LO}, f_s and images are shown in Figs. 2(a) and (b). The suppression of all images and IF & LO feedthrough, as shown by the hatched area in Fig. 2, can be confirmed. If 3rd order frequency conversion is used, the measurement range will be expanded up to 40GHz. Moreover, the measurement from DC becomes possible by replacing f_{LO1} in Eq. (12) to 18GHz.

MMICS

MMICs are developed for all the active elements shown in the hatched areas in Fig. 1. They are fabricated by the same process for higher levels of integration in the future. For the FETs, 0.25µm gate length hetero-junction FETs (nAlGaAs /nGaAs /InGaAs/GaAs, f_i=40 GHz, f_{max}=70 GHz) are applied. Co-planar waveguides are mainly used for the transmission lines because of their single plane metal fabrication
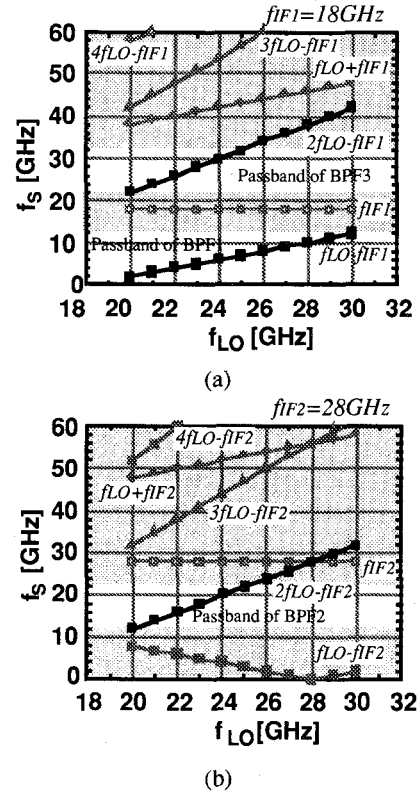

(a)

(b)

Fig. 2 The relationship of f_{LO}, f_s and images. (a) is at f_{IF1}. (b) is at f_{IF2}.

and their flexibile impedance characteristics, but thin film micro-striplines[3] are also used for line-cross-overs and bias distributions.

Figure 3 shows an equivalent circuit of the fundamental and harmonic mixer. An active power combiner composed of a common gate FET cell (CGF_s and CGF_{LO})[4] achieves ultra-wideband performances with newly developed negative feedback paths and a peaking element L_1. The negative feedback paths R_{Sfb} and R_{LOfb} control the peaking effect of the L_1 by using the FET's phase shift in high frequency to obtain a flat performance. The mixing mode of fundamental or 2nd order harmonics is selected by gate bias V_{gg} of the common source FET. Figures. 4 and 5 show a microphotograph and the results of conversion loss measurement. The measured conversion losses are 1.5-8.8 dB and 6.0-12.2 dB in the fundamental mode of 2-12 GHz f_s and 2nd order harmonic mode of 12-32 GHz f_s, respectively. This converter is also used for the down-converter in Fig. 1 due to the bandwidth. When the 2nd IF is 160 MHz, measured conversion losses are 9.4 dB and 4.8 dB at 18 GHz and 28 GHz input, respectively.

Figures 6 and 7 show an equivalent circuit and a microphotograph of the fabricated MMIC variable attenuator. This attenuator achieves a flat frequency response by means of a T-network composed of two pairs of shunt-FET-resistors with an inductive line between them [5]. The symmetrical

738

allocation of the shunt-FET-resistors reduces the discontinuously of the co-planar waveguide, and the inductive line compensates for bandwidth degradation at high attenuation and high frequency. Measurement attenuation of the MMIC attenuator varies from 2.8 dB to 30 dB in the 2-32 GHz range as shown in Fig. 8. The deviation of the level is within +/-0.5 dB at each 10 dB step of attenuation.

The T-network approach is also taken for the SPDT. Moreover, in the SPDT, subsidiary shunt FET-resistors are adapted for the gate electrodes of the series FET-resistors to improve high frequency isolation at the off port. Figure 9 shows an equivalent circuit of the MMIC SPDT. Since the subsidiary shunt FET-resistors S_9, S_{10}, S_{11} and S_{12} produce the reverse on/off states of each series FET-resistor, the signal leakage through the series-resistors' gate electrodes is shorted to ground in the off state. Figure 10 shows microphotographs of the MMIC SPDT. Measurement insertion loss and isolation are better than 3.9 dB and 33 dB, respectively, in the 2-32 GHz range, as shown in Fig. 11. When the coupling between co-planar waveguides is reduced by adding several via-holes [6], the isolation improves to 50 dB. Measured insertion loss and isolation of the SP3T are better than 3.3 dB and 34 dB, respectively, in the same frequency range.

Figure 12 shows a microphotograph of the MMIC distributed pre-amplifier. The gain cell consists of a cascade connection of FETs. Measured gain is 10 dB +/-2 dB in the 2-30GHz range. In particular, the insertion gain is 12 dB at 18 GHz and 11 dB at 28 GHz. An active lowpass filter that suppresses signal leakage of the 2nd LO was reported in the last MTT-S symposium.[7] Measured insertion gain is 11dB at the 2nd IF of 160 MHz, and the isolation at 18 GHz and 28 GHz is 40 dB and 32 dB, respectively.
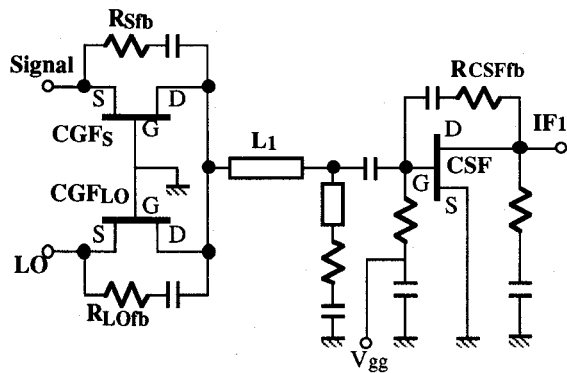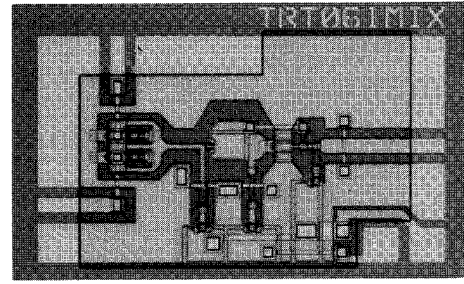

Fig. 4. Microphotograph of the fabricated MMIC fundamental and harmonic mixer.
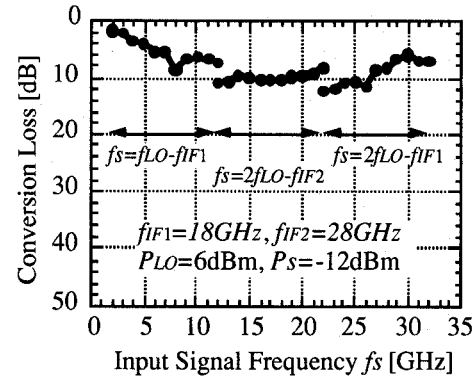

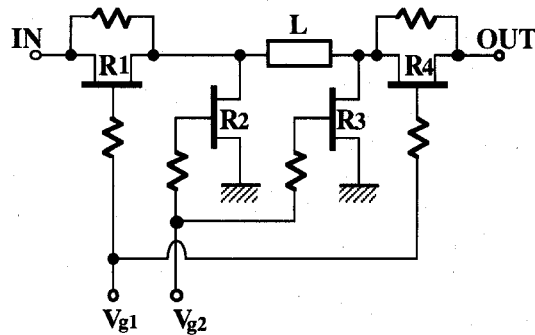Fig. 5. Measured conversion loss of the fabricated MMIC fundamental and harmonic mixer.

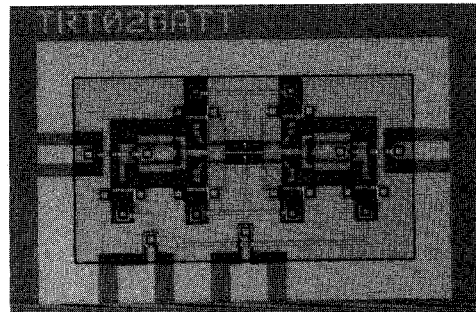Fig. 6. Equivalent circuit of the MMIC variable attenuator.

Fig. 3. Equivalent circuit of the MMIC fundamental and harmonic mixer.

Fig. 7. Microphotograph of the fabricated MMIC variable attenuator.
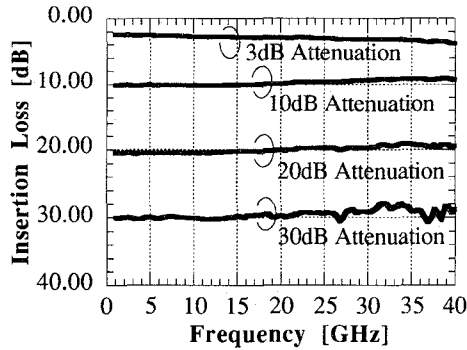
739

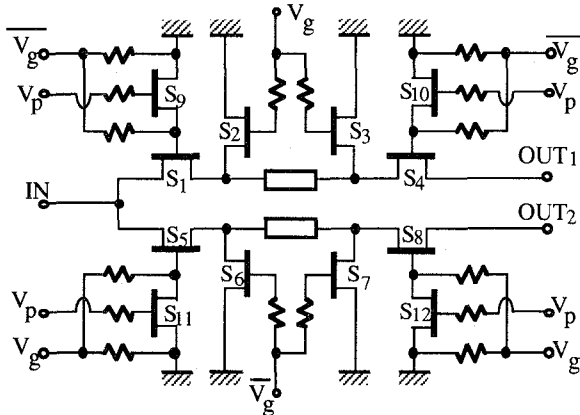Fig. 8. Measured performance of the MMIC variable attenuator.

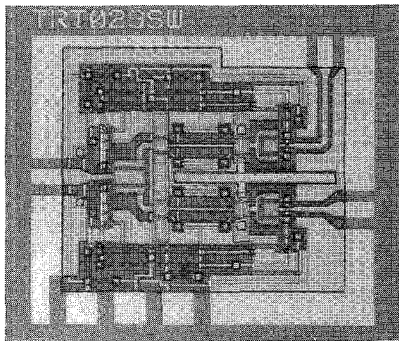Fig. 9. Equivalent circuit of the MMIC SPDT switch.

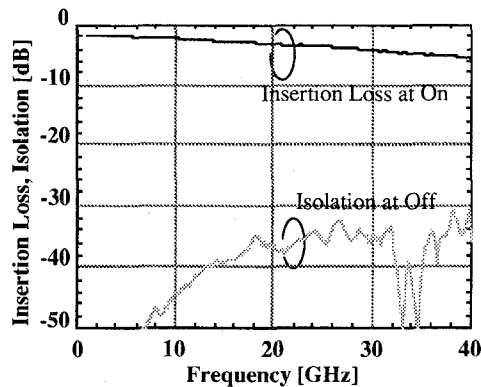Fig. 10. Microphotograph of the MMIC SPDT switch.

Fig. 11. Measured performance of the MMIC SPDT switch.
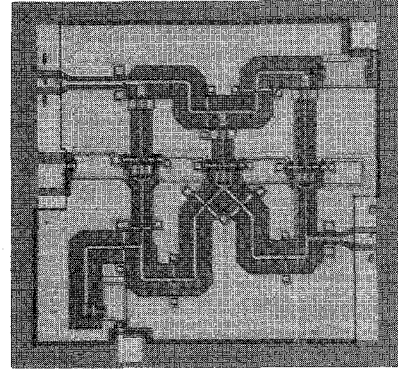

Fig. 12. Microphotograph of the MMIC distributed pre-amplifier.

CONCLUSION

A novel architecture and MMICs for an integrated front end of a spectrum analyzer have been proposed and demonstrated. The architecture and MMICs can achieve a wideband measurement range of 2-32 GHz with the 1st LO of 20-30 GHz, as well as allowing a probe configuration. Discounting filter factors, we estimate the total conversion loss to be 10-25 dB and image suppression to be better than 70 dBc at input power of -30 dBm. These values are comparable with those of the front ends of commercially available spectrum analyzers.

REFERENCE

[1] M. S. Shakouri, A. Black, B. A. Auld and D.M. Bloom, "500GHz GaAs MMIC sampling wafer probe," Electron. Lett., vol. 29, No. 6, pp. 557-558, Mar. 1993.

[2] R. Y. Yu, J Pusl, Y. Konishi, M. Case, M. Kamegawa and M. Rodwell, "A time domain millimeter-wave vector network analyzer," IEEE Microwave and Guided Wave Lett., vol. 2, No. 8, pp.319-321, Aug. 1992.

[3] T. Tokumitsu, T. Hiraoka, H. Nakamoto and T. Takenaka, "Multilayer MMIC using a 3μmx3-layer dielectric film strcture," in Digest of the IEEE MTT-S Symp., pp.831-834, June 1990.

[4] R. Soares, GaAs MESFET Circuit Design, Artech House, MA, 1988, pp.497-504.

[5] H. Kondoh, "DC-50GHz MMIC variable attenuator with a 30dB dynamic range," in Digest of the IEEE MTT-S Symp., pp.499-502, June 1988.

[6] S. G. Houng, T. Tsukii and M. J. Schindler, "60-70dB isolation 2-19GHz MMIC switches," in Digest of the IEEE GaAs IC Symp, pp.173-176, Oct. 1989.

[7] T. Takenaka, A. Miyazaki and H. Matsuura, "An MMIC active LC filter," in Digest of the IEEE MTT-S Symp., pp.609-612, May. 1994.